International Journal of Electrical and Computer Engineering (IJECE)
Vol. 8, No. 6, December 2018, pp. 4772~4780
ISSN: 2088-8708, DOI: 10.11591/ijece.v8i6.pp4772-4780

Metal-embedded SU-8 Slab Techniques for Low-resistance Micromachined Inductors

Manot Mapato[1], Prapong Klysuban[2], Thanatchai Kulworawanichpong[3], Nimit Chomnawang[4]
[1,3,4]School of Electrical Engineering, Suranaree University of Technology, Thailand
[2]Synchrotron Light Research institute, Ministry of Science and Technology, Thailand

Article Info

Article history:

Received May 22, 2017
Revised Jul 10, 2018
Accepted Jul 17, 2018

Keyword:

High aspect-ratio inductors
Metal-embedded SU-8 slab
Micro power inductors
Micromachined inductors
X-ray lithography

ABSTRACT

This work presents a new fabrication technique for micro power inductors by using metal-embedded SU-8 slab molding techniques. The proposed technique uses X-ray lithography to fabricate high-aspect-ratio LIGA-like microstructures in form of embedded structures in the SU-8 slab. This process was applied to fabricate an inductor's windings with an aspect ratio of 10, which can provide very low resistance but still preserve a small form factor and low profile. Inductors were designed as pot-core structures with overall heights of 370 µm and embedded with 250-µm-thick windings. From the advantage of metal embedded SU-8 slab techniques, 8 µm-thick permalloy core could be fabricated by electroplating around the winding in a single step that could help simplify the process. Four types of inductors were fabricated with 3, 5, 10, and 16 turns in the area of 1.8 to 9.5 mm2. The measured inductance was in the range of 70 nH to 1.3 µH at 1 MHz and DC resistance of 30–336 mΩ for 3–16 turns, respectively. The DC resistance of fabricated inductor was low, as expected, and showed good result compared with the results in literature.

Corresponding Author:

Manot Mapato,
School of Electrical Engineering,
Suranaree University of Technology,
111 University Avenue, NakhonRatchasima 30000, Thailand.
Email: manot.mapato@gmail.com

1. INTRODUCTION

Portable electronic devices have become a daily necessity. Over time, these fabricated devices have decreased in size and increased in efficiency. However, owing to their limited size, these devices have only single batteries supplying current to each circuit despite varying DC voltage requirements. Thus, the DC–DC converter circuit is an essential component of such devices and is determinant of device efficiency, and more efficient converter circuits have been continuously developed. The inductive-switching type circuit is currently very popular because of its provision of great efficiency with high power density. At present, the circuit is normally operated in the megahertz range [1]. In some literature, the circuits were designed to operate at a frequency of up to 100 MHz [2]; however, the efficiency at an extremely high frequency is still limited because of switching loss.

The advantage of working at a megahertz range could help decrease the inductance required. In addition, the inductor's size could be smaller and still be capable of being packed with ICs, thus facilitating in increasing the power density [3]. However, fabricating a highly efficient integrated inductor with a limited area has become a challenge because DC resistance plays an important role in inductor efficiency in a DC–DC converter circuit, as the majority of current flowing through the inductors is DC current. Thus, with the area constraint, it is hardly possible to fabricate the windings of a low-resistance inductor by using conventional thin film technology.

The windings of a micro-inductor are generally fabricated using a variety of techniques. Some techniques include sputtering, which could possibly lead to metal deposition at the submicron scale. This could result in an even higher resistance, which is more suitable for high-resistance applications [4]. Micromachining is another popular technique for three-dimensional microstructure fabrication. This technique fabricates a mold through bulk or surface micromachining and fills the mold with metal through electroplating [5], [6], and thus the fabricated structure could be as thick as the molds. Some researchers have fabricated an inductor directly onto the power ICs through silicon bulk micromachining by using reactive ion etching [7], [8]. This method can fabricate deep molds of up to 250 µm; however, silicon is not a good mold material for copper owing to their different thermal expansion coefficients, which could damage the mold. This method was improved by adding SU-8 photoresist to behave as a polymer wall inside the mold [5]; however, this could result in a double-molding process. Another fabrication process is the lithography process [9], [10] in which SU-8 molded fabrication was performed using the UV lithography technique, which can build a 100-µm-thick mold. However, this technique could not fabricate a high aspect-ratio structure. Generally, the aspect ratio at which the strucure can be built is only 1-3. Thus, this method still cannot achieve low-resistance winding with area limitation.

X-ray lithography is an excellent process for fabricating structures with high aspect ratios of more than 10. Further, SU-8 is a suitable material for molding because of its high X-ray sensitivity, which could help reduce exposure time. Therefore, this paper proposes the use of X-ray lithography for fabricating a micro-inductor for DC–DC converter application. Per the authors' research, this is the first study to consider this process for fabricating the windings of a DC inductor with an aspect ratio of up to 10. This could help in the fabrication of very low-resistance windings while preserving a small form-factor and low profile. The overall process was performed using the "metal-embedded SU-8 slab techniques," which fabricate inductor windings embedded in an SU-8 slab in a substrate-less form, such as a silicon wafer. The metal-embedded slab would allow the fabrication of additional structures on both sides. This process was used to fabricate the inductor's core by electroplating a magnetic core around the winding with single steps, which could help to simplify the process and reduce cost. The whole fabrication process is detailed in section 3. Moreover, section 4 presents the characteristics of the inductors, which include DC resistance, AC resistance, inductance, and saturation current.

2. INDUCTOR GEOMETRY

2.1. Inductors Winding

In this study, inductors were designed as a pot-core structure owing to its small form factor, low profile, and suitability for batch fabrication. This structure has a rectangular spiral winding, as shown in Figure 1. The windings were designed with a width of 25 µm, which is the smallest resolution at which the UV mask could be printed with the equipment used in our experiments. Regarding the height of the winding, it was designed with an aspect ratio of 10 and was fabricated at the DXRL laboratory of the Synchrotron Light Research Institute, Thailand. Thus, 250-µm-thick windings were designed. From this structure, the winding length could be calculated using the analytical model, as presented in equation (1), and it was sequentially substituted in equation (2) to calculate the winding resistance. By considering the dimension of the structure, the resistance of the inductors with windings of 3, 5, 10, and 16 turns could be calculated, as shown in Table 1. The calculated resistance of the inductor was in the range of 27–270 mΩ.

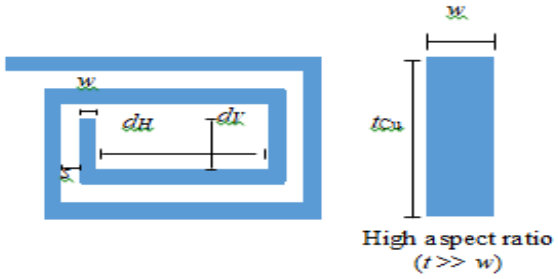

Figure 1. Copper winding dimension and parameters for resistance calculation

$$l_{Cu} = \left[2 \cdot n \cdot d_V + (2n^2 - n) \cdot (w + s)\right] + \left[2 \cdot n \cdot d_H + (2n^2 - n) \cdot (w + s)\right] + 4nw \quad (1)$$

$$R_{DC} = \frac{\rho_{Cu}}{t_{Cu} \cdot w}\left[\left[2 \cdot n \cdot d_V + (2n^2 - n) \cdot (w+s)\right] + \left[2 \cdot n \cdot d_H + (2n^2 - n) \cdot (w+s)\right] + 4nw\right] \quad (2)$$

where

l_{Cu} : copper winding length

R_{DC} : winding resistance

n : number of turns

d_{inV} : inner space width

d_{inH} : inner space long.

s : space between windings

w : conductor width

t_{Cu} : conductor height

ρ_{Cu} : esistivity of material.

Table 1. Calculated Resistance of Inductors' Windings

Number of turns (turn)	Coil Thickness (μm)	Coil width (μm)	Resistance (mΩ)
3	250	25	27.0
5	250	25	51.1
10	250	25	132.3
16	250	25	269.4

2.2 Magnetic core

Permalloy ($Ni_{80}Fe_{20}$) was chosen as the magnetic core material. Owing to its high permeability, high saturation flux density [11], and suitability for microfabrication, the material could be formed through electroplating. The current density of 5 mA/cm^2 was optimized for electroplating, as the maximum current does not yield bubbles inside the material during electroplating, thus achieving a smooth surface. At this current density, the deposition rate of metal was 8 μm/h. The magnetic characteristic of the material was tested [12], and it has a permeability of 550, saturation flux density of 0.75 Tesla, conductivity of 5.66×10^6 S/m, and calculated skin depth at 1 MHZ of 8 μm. However, as its high conductivity easily led to eddy current loss, the magnetic core was required to be designed with a thickness lesser than or equal to the skin depth at the operating frequency to avoid power loss. Thus, the inductor core, which was designed to be no more than 8-μm thick, could avoid power loss from eddy current when the inductor operated at a frequency of approximately 1 MHz.

The inductor structure was designed as a pot-core type which was surrounded by a magnetic core, as shown in Figure 2. This structure was suitable for applying to the fabrication process of metal-embedded SU-8 slab because a magnetic core can be simultaneously electroplated around the winding in a single step, which could help simplify the process. Furthermore, the advantages of this structure include thermal sink [13], [14] and flux leakage reduction because of the presence of the metal core around the inductor structure. According to this design, the winding was 250-μm thick, and the whole structure height including insulation layer and magnetic core was less than 400-μm thick, which is good in on-chip inductors for micro power converter applications.

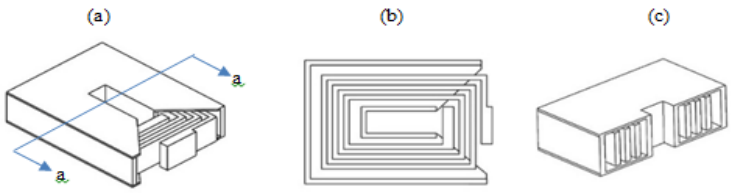

Figure 2. Model of a 3-turn inductor with 250-μm-thick winding: (a) 3D model,(b) Top view cross-section, and (c) a–a cross-section

3. INDUCTOR FABRICATION

3.1. Metal-embedded SU-8 slab fabrication technique

The metal-embedded SU-8 slab fabrication technique is a novel process for fabricating an inductor winding that includes surface micromachining on substrate, then the substrate is removed. The finished sample could be used to build additional structures on both sides, and this structure could be mounted directly onto ICs. The X-ray lithography process was used to fabricate a high aspect-ratio mold. The process initiated from the fabrication of the winding by coating an SU-8 photoresist with 300 µm thickness on a Graphite substrate, and then soft baking at 95 °C for 13 h. The sample was cooled to 25 °C at a rate not faster than 0.5 °C/min to avoid sample deflection caused by the stress inside the thick film. A 50-µm-thick silver mask was used as the X-ray mask, exposed to X-rays through a silver mask with a power of 22 J/cm^3, and soft baked for 20 min. The exposed sample was developed using the SU-8 developer solution for 2 h, and then rinsed with acetone and deionized water to clean residual SU-8 in the mold. The sample was hard baked and plasma cleaned using argon; this clean and dry sample could allow efficient electroforming inside the SU-8 mold.

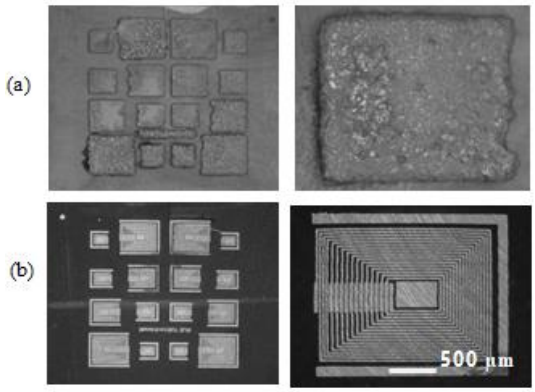

Figure 3. (a) Electroplated and (b) polished over-filled copper windings embedded in the SU-8 mold

For the electroplating process, the mold was filled with electroplated copper by using two current steps: 30 mA/cm^2 for 10 min to reduce the nonuniformity of the copper deposited on the graphite substrate and 10 mA/cm^2 until the copper overfilled the mold, as shown in Figure 3(a). Mechanical polishing was performed for removing the overfilled copper, as shown in Figure 3(b), as well as the graphite substrate. Figure 4 shows the cross-sectional view of the process flow and Figure 5 shows the transparent embedded copper winding inside the SU-8 slab.

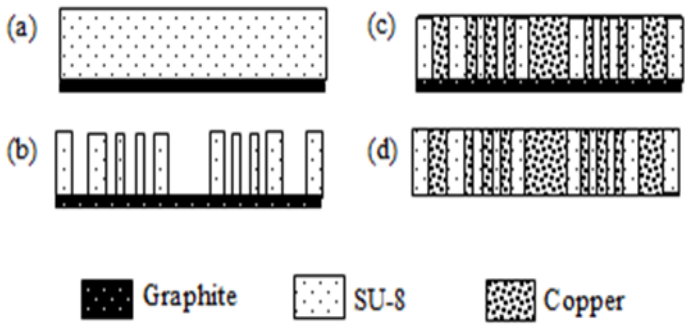

Figure 4. Cross-sectional view of the process flow of X-ray lithography molding techniques for thick-coil fabrication: (a) 300-µm-thick SU-8 on graphite substrate; (b) X-ray exposed and developed; (c) Copper electroplating and polishing; (d) graphite substrate is removed

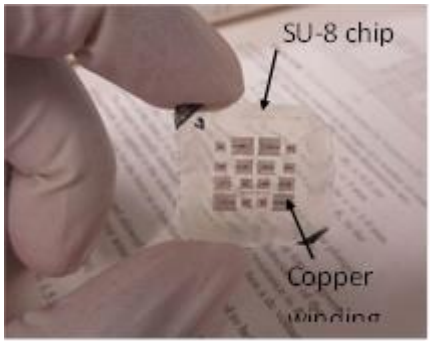

Figure 5. Transparent 250-µm-thick SU-8 slab with copper winding embedded

3.2. Magnetic core fabrication

The SU-8 and dry film were used as photosensitive materials, and the inductor's core was fabricated using UV lithography, electroplating, sputtering, and material lift-off techniques. The fabrication process was initiated by spin coating a 50-µm-thick SU-8 photoresist on an SU-8 slab, and then soft baking at 95 °C for 10 min. Next, the photoresist was exposed to UV with an energy of 255 mJ/cm^2 through the printed UV mask. After soft baking again, the sample was developed in the SU-8 developer. This process was repeated on the other side to create an etching-protect layer on both sides and used as an insulator between the windings and magnetic core, as shown in Figure 6(b). Chemical etching was performed to remove copper in the core area by using 50% Nitric acid. After etching, the copper inside the core area was removed, as shown as Figure 6(c).

The dry-film photoresist was used as the sacrificial layer under the copper seed layer to define the core's deposition area. A dry-film photoresist was then coated on both sides of the SU-8 slab, and was then exposed to UV with 25-mJ/cm^2 energy; it was then developed using the dry-film developer to remove the unexposed film, as shown in Figure 6(e). The copper seed layer was deposited on the whole sample through DC sputtering, as shown in Figure 6(f), and then lifted off the dry film by using acetone. The sample was ready for magnetic-core electroplating, as shown in Figures 6(g) and 7(b). All the cores were connected together by using a copper track for batch electroplating, as shown in Figure 8. Permalloy electroplating was performed with a current density of 5 mA/cm^2 by using a NiFe batch solution. This condition can provide a deposition rate of 8 µm/h. An electroplated sample is shown in Figure 8.

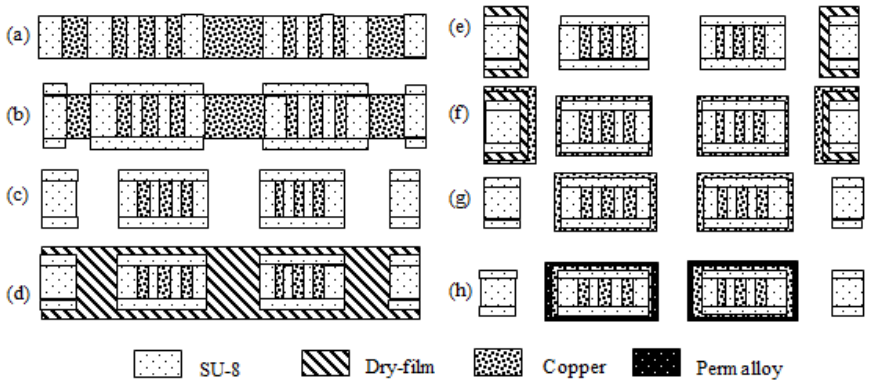

Figure 6. Cross-sectional view of process flow of metal embedded SU-8 slab techniques for integrated micro inductors: (a) copper-embedded SU-8 slab; (b) spin coating 50 µm of SU-8 photoresist and patterning of SU-8 on both sides; (c) removing copper; (d) coating dry-film photoresist on both sides; (e) patterning dry film; (f) deposit copper seed layer through sputtering; (g) lifting of dry film; (h) electroplating permalloy and then removing SU-8 on the bonding pad through plasma etching.

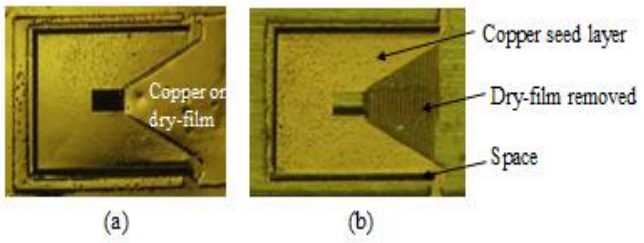

Figure 7. The fabricated 16-turn micropower inductors embedded in SU-8. (a) Sputtered copper seed layer (b) Lift-off dry film and copper

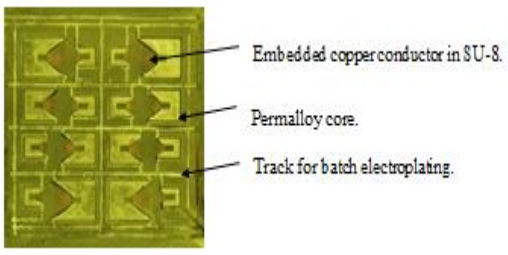

Figure 8. Batch fabrication of micropower inductors embedded in SU-8 slabs

After fabrication, the SU-8 over-coated on the bonding pad was removed through plasma etching, and then rinsed with sulfuric acid to remove copper oxide to clean the bonding pad and ready it for wire bonding. Inductors have an overall height of 370 µm, including that of the 250-µm-thick winding, 100 µm of

insulator, and 16 µm of magnetic core. Figure 9 shows completely fabricated samples and cross-sections of the fabricated samples.

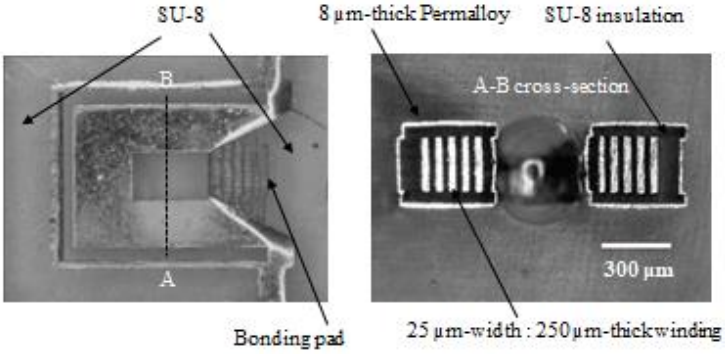

Figure 9. The fabricated 5-turn micro power inductors and cross-section

4. RESULT AND DISCUSSION

The DC resistance of the fabricated inductors was tested using a four-probe measurement technique; the measured DC resistances are in the range of 29.8–335.6 mΩ for the inductors with 3–16 turns, respectively, as shown in Table 2. The measured value is close to that calculated using equation (2); some deviations were observed owing to the UV mask's dimension error because the limitation of the printer was close to the structure size. By measuring the fabricated inductor's winding width, the average width was determined to be 23 µm. As the design was set at 25 µm, it resulted in a higher inductor resistance than that of the design, especially for the 16-turn inductor with the maximum resistance deviation. However, the inductor fabricated as a high aspect ratio structure had low DC resistance, as expected, and its resistance can be ranked in the low-resistance group compared to literature that lists resistance in a range of 9 mΩ–4.6 Ω [3], [5]–[7], [10], [11], [16]–[19].

Table 2. Measured and Calculated DC Resistances of the Fabricated Inductors

Inductor type	$R_{DC\ Calc}$ (mΩ)	$R_{DC\ meas}$ (mΩ)	Area (mm^2)	Conductivity/Area (S/mm^2)
3 turns	27.0	29.8	1.8	18.64
5 turn	51.1	51.1	2.34	8.36
10 turn	132.3	148.6	5.25	1.28
16 turn	269.4	335.6	9.45	0.31

High-frequency characterization was performed using a vector network analyzer Agilent 8650ES, and one port scattering (S_{11}) measurement was conducted in the frequency range of 30 kHz to 1 GHz while the parasitic capacitance of the DUT pad and connector were de-embedded using the admittance matrix method [15]. The self-resonance frequency was not observed in the frequency range of 30 kHz to 1 GHz for 3-10-turn inductors but was observed at 800 MHz for the 16-turn inductor. Thus, the results of self-resonance can be ignored because the inductor was designed to work at the frequency of approximately 1 MHz. The measured S_{11} value was considered to calculate the inductance value by using the L–R Series Model. In Figure 10(a), the inductance was a function of frequency and slightly decreased with the increase in frequency because of the decrease in permeability. At frequencies higher than 1 MHz, the inductance value decreased significantly because the skin-depth value of the magnetic core was higher than the thickness of the core. Thus, the inductance value subsequently decreased according to the decrease in the cross-sectional area of magnetic core.

Figure 10(b) shows the inductor resistance as a function of frequency, representing DC and AC winding losses and core loss. When considering the frequency range below 1 MHz, the inductor resistance value increased with frequency because of the skin depth of the high aspect ratio winding; however, it increased rapidly for frequencies higher than 1 MHz. This represents the Eddy current loss in the magnetic core because its thickness was greater than the skin depth. Thus, in case a future device requires operation at

a higher frequency, the thickness of the magnetic core could be reduced, or the core could be fabricated in a laminate pattern to reduce loss and thus help increase inductor efficiency.

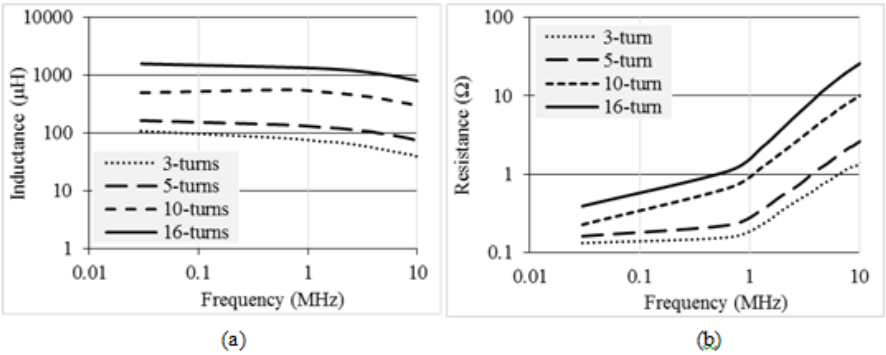

Figure 10. The measured inductance and AC resistance in a frequency range of 30 kHz to 10 MHz

Magnetic core saturation was demonstrated by biasing the DC current in the range of 0 to 500 mA with 1-MHz frequency modulation. Figure 11 shows the inductance values as a function of biasing current. The inductance of all inductors decreased with the increase of the biased current; this represents the beginning of magnetic core saturation, at which the inductance value was reduced by 20 % of the initial inductance. The result showed that the saturated currents of all the inductors were approximately 110 mA, which was rather low. The low saturation current resulted from the un-gapped core designed. In case of a design demand of higher current, a gap could be added or re-design the magnetic core.

Figure 12(a) shows a comparison of the fabricated inductors against those in literature according to inductance and DC resistance. The inductance values were comparable to those of other researches which are in a range of 100 nH–1 µH. Regarding the resistance, their values can be ranked in the low resistance group, but still higher than [5], which has the lowest resistance at 9.1 mΩ. However, if we consider the inductor's area, the inductors in this research have area in a range of 1.8 mm^2–9.4 mm^2 while the inductors in other researches have area in a range of 4 mm^2–304 mm^2. So, the area is another comparison factor that should consider.

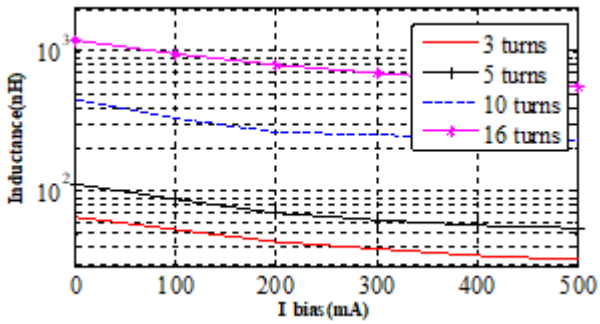

Figure 11. Measured inductance as a function of DC bias current at 1 MHz

In Figure 12(b), the resistances were converted to conductivity and divided by the footprint area, showing that higher conductivity in a small area was achieved for DC inductor fabrication. From the result, the inductors from this research show good conductivity when measured by area, and are comparable to the best results from other literature. The low resistance per area resulting from the high aspect ratio structure could help to minimize DC resistance even within a small footprint. In summary, the inductors fabricated using the high aspect ratio associated with the process of metal-embedded SU-8 slab techniques yield good results including low-resistance, high inductance, and small form factor. However, they still need an improvement of the saturation current.

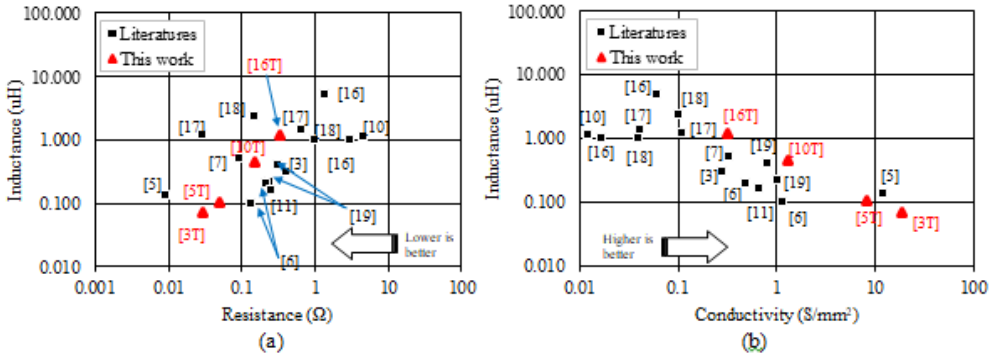

Figure 12. Inductance and resistance of fabricated inductors compared to literature values: [3], [5]-[7], [10], [11] and [16]-[19]: (a) inductance and resistance (b) inductance and conductivity per area

5. CONCLUSION

Micromachined inductors for DC–DC converter application were fabricated using metal-embedded SU-8 slab techniques. The winding was fabricated through a X-ray lithography process to fabricate the inductors' windings with a high aspect ratio of 10. This structure could help minimize the DC resistance while preserving a small form factor and low profile. With the advantage of metal-embedded SU-8 slab techniques, the magnetic core can be deposited around the windings at once and could help simplify the process and reduce cost. As the result, the measured DC resistance showed low DC resistance as expected, lower than literature values, when factored against the inductor area. The inductance showed results comparable to the literature, but the saturation current was rather low because the magnetic core was configured as ungapped. For future research, the core structure could be developed to acquire higher saturation current by fabricating with a lamination or using a material that could support higher frequency.

6. ACKNOWLEDGEMENTS

This research is fully supported by Synchrotron Light Research Institute (Public Organization), Thailand.

REFERENCES

[1] N. Wang, *et al.*, "High Frequency dc-dc Converter with Co-packaged Planar Inductor and Power IC," in 2013*Electronic Components & Technology Conference, 2013.*, pp. 1946-1952

[2] G. Schrom, *et al.*, "A 100MHz Eight-Phase Buck Converter Delivering12A in 25mm2 Using Air-Core Inductors," *Applied Power Electronics Conference, APEC 2007- Twenty Second Annual IEEE*, pp. 727-730, Feb 2007.

[3] N. Wang, *et al.*, "Micro-inductors integrated on silicon for power supply on chip," *Journal of Magnetism and Magnetic Materials, 2007*, pp. 233-237.

[4] P. Deekla, *et al.*, " Al Microheater and Ni Temperature Sensor Set based-on Photolithography with Closed-Loop Control," *International Journal of Electrical and Computer Engineering*, vol. 5, No 4, pp. 849-858, Aug 2015.

[5] M. Wang, *et al.*, "Silicon molding techniques for integrated power MEMS inductors,"*Sensors and Actuators A: Physical, 2011*,vol. 166, pp. 157-163.

[6] T. O'Donnell, *et al.*, "Microfabricated Inductors for 20 MHz Dc-Dc Converters," in *Applied Power Electronics Conference and Exposition, 2008.APEC 2008. Twenty-Third Annual IEEE*, 2008, pp. 689-693.

[7] B. Orlando, *et al.*, "Low-Resistance Integrated Toroidal Inductorfor Power Management," *IEEE Transactions on Magnetics*, vol. 42, pp. 3374-3376, 2006.

[8] M. Wang, *et al.*, "SU8 Enhanced High Power Density MEMS Inductors," in 2008 *Proc. of the 34th Annual Conference of the IEEE Industrial Electronics Society 2008.*, pp. 1946-1952

[9] E. Brandon, *et al.*, "Fabrication and Characterization of Microinductors for Distributed Power Converters," *IEEE Transactions on Magnetics*, vol. 39, pp. 2049-2056, Jul 2003.

[10] D. Sadler, *et al.*, "Micromachined Spiral Inductors Using UV-LIGATechniques," *IEEE Transactions on Magnetics*, vol. 37, pp. 2897-2899, Jul2001.

[11] N. Wang, *et al.*, "High-frequency Micro-machined Power Inductors," ," *Journal of Magnetism and Magnetic Materials*, vol. 290-291, part 2, pp. 1347-1350, Apl 2005.

[12] O. Caltun, *et al.*, "Initial permeability, hysteresis and total losses measurements," in *AnaleleStiintifice-FizicaStarii Condensate 2000*, pp. 56-60.
[13] Y. Benhadda, *et al.*, " Thermal Behavior of an Integrated Square Spiral Micro Coil," TELKOMNIKA *Indonesian Journal of Electrical Engineering and Computer Science*, vol. 14, No 2, pp. 250-265, May 2015.
[14] M Derkaoui, A Hamid, T Lebey, R Melati. *Design and Modeling of an Integrated MicroTransformer in a Flyback Converter*. TELKOMNIKA. 2013; 11(4): 669-682.
[15] S. Linder, "S-parameter techniques for faster, more accurate network design," *HP application note 95-1*, Hewlett Packard 1996.
[16] F. Sato, *et al.*, "All-in-One Package Ultracompact MicropowerModule Using Thin-Film Inductor," *IEEE Transactions on Magnetics*, vol. 40, pp. 2029-2031, Jul 2004.
[17] J. W. Park and Mark G. Allen, "Ultralow-Profile Micromachined Power Inductors With Highly Laminated Ni/Fe Cores: Application to Low-Megahertz DC–DC Converters," *IEEE Transactions on Magnetics*, vol. 39, pp. 3184-3186, Sep 2003.
[18] K. H. Kim, *et al.*, "A Megahertz Switching DC/DC ConverterUsing FeBN Thin Film Inductor," *IEEE Transactions on Magnetics*, vol. 38, pp. 3162-3164, Sep 2002.
[19] C. H. Ahh and M.G. Allen,"Micromachined Planar Inductors on Silicon Wafers for MEMS Applications," *IEEE Transactions on Industrial Electronics*, vol. 45, pp. 866-876, Dec 1998.

BIOGRAPHIES OF AUTHORS

Manot Mapato received his B.Eng. and M.Eng. from Suranaree University of Technology, Nakhon Ratchasima, Thailand in 2005 and 2007, respectively, both in Electrical Engineering. With financial support from the Synchrotron Light Research Institute (Public Organization), he is currently working toward the Ph.D. degree in the School of Electrical Engineering, Institute of Engineering, Suranaree University of Technology. His research interests include X-ray lithrography application, micro-sensor, micro-electronics devices and embedded control system.

Prapong Klysubun received his B.Sc. (Hons) degree in physics from Chulalongkorn University, Bangkok, Thailand, in 1996, and his M.Sc. and Ph.D. degrees in physics from Virginia Polytechnic and State University (Virginia Tech) in 1998 and 2002, respectively. After graduation, he started working as a researcher at Synchrotron Light Research Institute (formerly known as National Synchrotron Research Center). He is currently serving as an Assistant Director and the Director of Accelerator Technology Division of SLRI. His research interests include accelerator physics, particle beam dynamics, and applications of synchrotron radiation.

Thanatchai Kulworawanichpong received his B.Eng. from Suranaree University of Technology, Nakhon Ratchasima, Thailand in 1998 and his M.Eng. from Chulalongkorn University, Bangkok, Thailand in 2000, both in Electrical Engineering. He also got his Ph.D. from the University of Birmingham, England, 2004. His employment experience started with teaching assistant in 1998 at School of Electrical Engineering, Suranaree University of Technology. In 2000, he was promoted to be a full-time lecturer of the same school. Again, he was promoted to be an associate professor of electrical engineering as his current position up-to-now. He became a member of several well-known academic societies, such as, WSEAS, IEEE, IET, IEEJ, WASET, IASTED, etc. Also he has usually served these societies as their referee for reviewing submitted papers to their journals. His special fields of interest included electrical machines, power electronic control and drives, soft computing, modeling and simulation with advanced numerical techniques, and electrical power system analysis.

Nimit Chomnawang received the B.Eng. degree in instrumentation engineering from King Mongkut's Institute of Technology, Ladkrabang, Thailand, in 1993, the MS degree in biomedical engineering from Virginia Commonwealth University in 1999, and MS and PhD degrees in electrical engineering from Louisiana State University in 2001 and 2002, respectively. Since 2002, he has been a lecturer at the School of Electrical Engineering, Suranaree University of Technology, Thailand. His research interests include microfabrication, MEMS, biomedical instrumentation, and embedded automation.